SUPPLEMENT TO "A NEW PARAMETRIZATION OF CORRELATION MATRICES"

(*Econometrica*, Vol. 89, No. 4, July 2021, 1699–1715)

ILYA ARCHAKOV
Department of Statistics and Operations Research, University of Vienna

PETER REINHARD HANSEN
Department of Economics, University of North Carolina

WE PRESENT four sets of supplementary results: (1) The finite-sample properties of $\hat{\gamma}$ when C has a Toeplitz structure. (2) The finite-sample properties of $\hat{\gamma}$, when C has general (randomly generated) structure. (3) The Jacobian $\partial\varrho/\partial\gamma$ for two correlation matrices. One with a Toeplitz structure, and one based on the empirical correlation matrix for daily returns on 10 industry portfolios. (4) Software implementations of $C(\gamma)$ that reconstructs C from γ for Julia, Matlab, Ox, Python, and R.

APPENDIX S.1: FINITE-SAMPLE PROPERTIES OF $\hat{\gamma}$ WHEN C HAS A TOEPLITZ STRUCTURE

Consider the following Toeplitz structure for the correlation matrix:

$$C = \begin{pmatrix} 1 & \rho & \rho^2 & \cdots & \rho^{n-1} \\ \rho & 1 & \rho & \cdots & \rho^{n-2} \\ \rho^2 & \rho & 1 & \cdots & \rho^{n-3} \\ \vdots & \vdots & \vdots & \ddots & \vdots \\ \rho^{n-1} & \rho^{n-2} & \rho^{n-3} & \cdots & 1 \end{pmatrix}. \tag{S.1}$$

The structure in C is here regulated by a single parameter, $\rho \in (-1, 1)$. The variables are uncorrelated when $\rho = 0$, and the pairwise correlation increases, as ρ increases from 0 to 1. The correlation matrix becomes near-singular for ρ close to 1.

We simulate $X_t \sim \text{i.i.d.}N_n(0, C)$, $t = 1, \ldots, T$, where C is given from (S.1) and T is a sample size. We then use X_t, $t = 1, \ldots, T$, to compute $\hat{C}$, from which we obtain the vector of correlations, $\hat{\varrho} = \text{vecl}(\hat{C})$, the corresponding vector of Fisher transformed correlations, $\hat{\phi}$, and $\hat{\gamma} = \gamma(\hat{C})$. Figure S.1 shows the finite-sample distributions for the first elements of these vectors, $\hat{\varrho}_1$, $\hat{\phi}_1$, and $\hat{\gamma}_1$, when $n = 3$. The Figure is based on 100,000 simulated samples of size $T = 40$, where $\rho = 0.9$. The left panels illustrate the well-known results that the finite-sample distribution of the empirical correlation is poorly approximated by a Gaussian distribution, especially if the true correlation is close to one. In this case, $\varrho_1 = 0.9$. The middle panels present the analogous results for the vector of elementwise Fisher transformed correlations, $\hat{\phi}_1$, and the right panels present the results for $\hat{\gamma}_1$. The finite-sample distribution of both $\hat{\phi}_1$ and $\hat{\gamma}_1$ are well approximated by the Gaussian distribution. This was expected for the Fisher transformation, $\hat{\phi}_1$, but somewhat unexpected

Ilya Archakov: iarchakov@gmail.com
Peter Reinhard Hansen: reinhardhansen@gmail.com

 https://doi.org/10.3982/ECTA16910

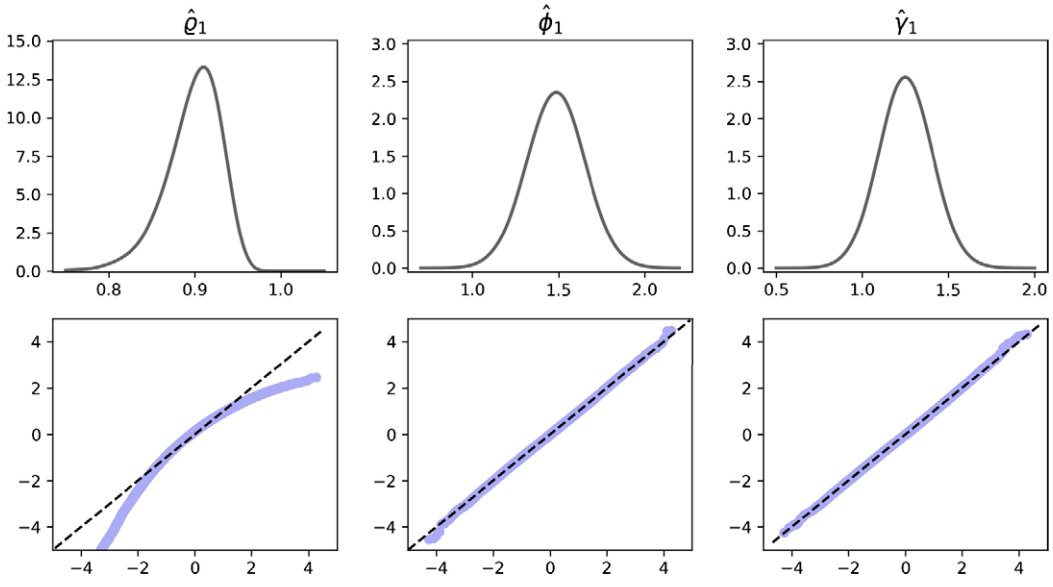

FIGURE S.1.—The finite-sample distribution (upper) and Q–Q-plots (lower) of the first elements of the vectors $\hat{\varrho}$, $\hat{\phi}$, and $\hat{\gamma}$. Results for the marginal distributions of $\hat{\varrho}_1$, $\hat{\phi}_1$, and $\hat{\gamma}_1$, are in the left, middle, and right panels, respectively. The simulation design has $\hat{C}$ computed from $T = 40$ independent vectors that are distributed as $N_3(0, C)$, where C has the Toeplitz structure (S.1) with $\rho = 0.9$. The results are based on 100,000 simulations. The Q–Q plots are the quantiles of the standardized empirical distribution plotted against quantiles of the standard normal distribution.

for $\hat{\gamma}_1$. In fact, the Q–Q plots indicate that the Gaussian approximation is slightly better for $\hat{\gamma}$ than for $\hat{\phi}$. A plausible explanation for this discrepancy is that the individual Fisher transformed correlations are subject to cross restrictions.

In Figure S.2, we compare the finite-sample variance and skewness of $\hat{\varrho}_1$, $\hat{\phi}_1$, and $\hat{\gamma}_1$ computed using 100,000 simulated samples of sizes $T = 40$ and $T = 100$, for $\rho \in [0, 1)$. The upper panels show that the new parametrization does not preserve the variance-stabilizing property for the entire range of ρ, but it does appear to eliminate skewness, as shown in the lower panels.

Figures S.1 and S.2 suggest that the marginal distributions of $\hat{\gamma}$ are well approximated by a Gaussian distribution. Next, we focus on the interdependence between the elements within the vectors $\hat{\varrho}$, $\hat{\phi}$, and $\hat{\gamma}$. Based on the same simulation design, we present the three bivariate distributions that emerge from the three empirical correlations, the corresponding three Fisher transformed correlations, and the three elements of $\hat{\gamma}$. Contour plots (nonparametrically estimated) for these bivariate distributions are given in Figure S.3. The dependence between empirical correlations (left column) is evident, and this cross dependence carries over to the element-wise Fisher transformed correlations (middle column). In contrast, the dependence between the elements of $\hat{\gamma}$ is much weaker (right column). The contour plots for the bivariate distributions of $\hat{\gamma}$ resemble those of a bivariate Gaussian distribution with little correlation between the two variables. This highlights an unanticipated and, potentially, very useful property of the new parametrization. We investigate the correlation between the elements of $\hat{\gamma}$ in greater details next.

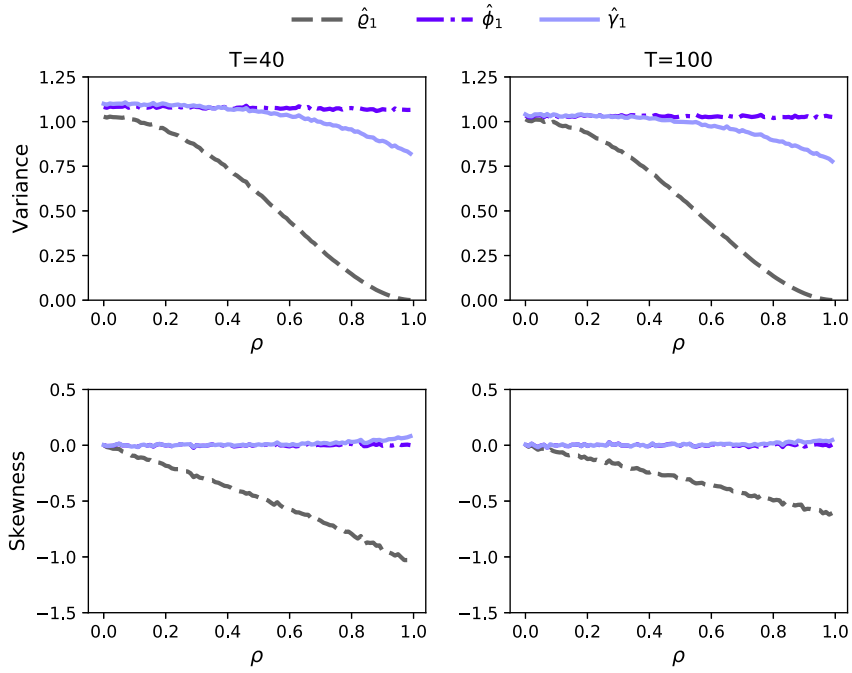

FIGURE S.2.—The finite-sample variance (upper panels) and finite-sample skewness (lower panels) of the empirical correlations for each of the elements of: $\sqrt{T}(\hat{\varrho} - \varrho)$, (dotted grey lines), $\sqrt{T}(\hat{\phi} - \phi)$ (dash–dotted violet lines), and $\sqrt{T}(\hat{\gamma} - \gamma)$ (solid amethyst lines) for $T = 40$ (left column) and $T = 100$ (right column), as a function of ρ. The results are based on (3×3) sample correlation matrices, computed from $X_t \sim$ i.i.d. $N_3(0, C)$, $t = 1, \ldots, T$, where C has the Toeplitz structure gives in (S.1). The results are based on 100,000 simulations.

Now we study the finite-sample correlations between the elements of $\hat{\phi}$ and $\hat{\gamma}$ for matrices of higher dimensions. We let

$$R_{\phi,T}(\rho) = \text{corr}(\hat{\phi}) \quad \text{and} \quad R_{\gamma,T}(\rho) = \text{corr}(\hat{\gamma}),$$

denote the finite-sample correlation matrices for $\hat{\phi}$ and $\hat{\gamma}$, and compute measures of dependence from $R_{\phi,T}(\rho)$ and $R_{\gamma,T}(\rho)$. The largest eigenvalue of the correlation matrix, R, is an approximate measure of the average correlations in R. Thus, $\lambda_{\max}(R) = 1$ is the lowest possible value achieved if and only if $R = I$, when all correlations are zeroes. In the other extreme, when all variables are nearly perfectly correlated, $\lambda_{\max}(R)$ approaches its upper limit. A natural measure of correlatedness in R is given by

$$\psi(R) = \big(\lambda_{\max}(R) - 1\big)/(d - 1),$$

because $\lambda_{\max}(R) \simeq 1 + (d - 1)\bar{r}$, where $\bar{r}$ is the average correlation of R, see Morrison (1967), who derived the approximation when the correlations are nonnegative and similar in value; see Friedman and Weisberg (1981) for a more general interpretation.

For simulations, we consider Toeplitz correlation matrices of dimensions, $n = 10$, 20, and 40, and with ρ ranging from 0 to 0.99. For each configuration of n and ρ, we simulate 10,000 realizations of $\hat{\phi}$ and $\hat{\gamma}$ using the sample size $T = 100$ and compute their corresponding correlation matrices, $R_{\phi,T}(\rho)$ and $R_{\gamma,T}(\rho)$. The dimension of these correlation matrices are given by 45×45 ($n = 10$), 190×190 ($n = 20$), and 780×780 ($n = 40$), since

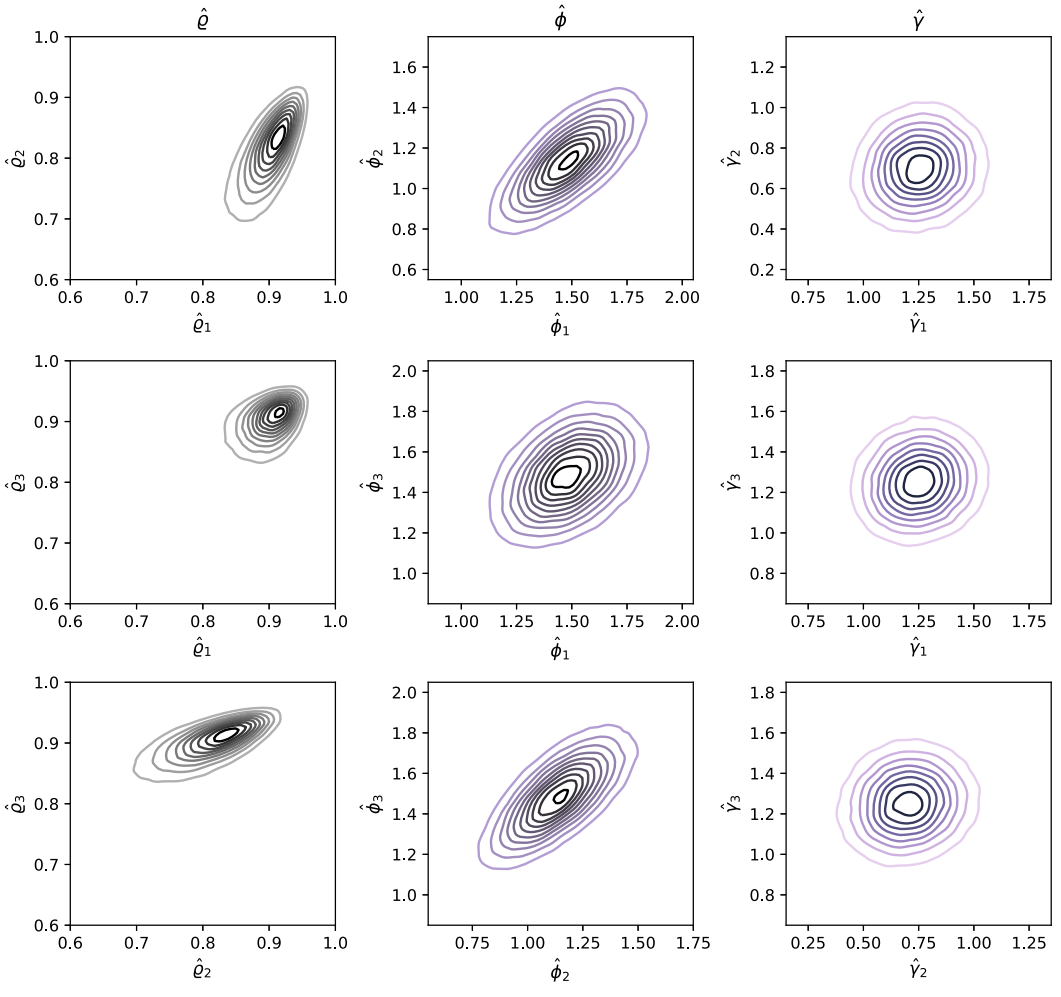

FIGURE S.3.—Contour plots of the bivariate distributions. The left panels are those for the empirical correlations, $\hat{\varrho}$, the middle panels are for the elementwise Fisher transformed correlations, $\hat{\phi}$, and the right panels are those for the new parametrization of the correlation matrix, $\hat{\gamma}$. The contour plots are based on 100,000 random draws, where each of the correlation matrices were based on $T = 40$ i.i.d. variables distributed as $N_3(0, C)$, where C has the structure in (S.1) with $\rho = 0.9$.

$d = n(n-1)/2$. Finally, we are able to obtain the correlation-measures, $\psi(R_{\phi,T}(\rho))$ and $\psi(R_{\gamma,T}(\rho))$, for each given n and ρ.

The results are reported in Figure S.4. Results for the elementwise Fisher transforms, $\hat{\phi}$, are in the left panels, and the corresponding results for the new parametrization, $\hat{\gamma}$, are in the right panels. The black solid lines present the eigenvalue-based correlation-measures, $\psi(R_{\phi,T}(\rho))$ and $\psi(R_{\gamma,T}(\rho))$, as a function of ρ. Besides reporting $\psi(R_{\phi,T}(\rho))$ and $\psi(R_{\gamma,T}(\rho))$, we also report the smallest and largest correlation elements from $R_{\phi,T}(\rho)$ and $R_{\gamma,T}(\rho)$ as well as their 10% and 90%-quantiles, to get a sense of the overall dispersion of the corresponding correlation coefficients. The lightly shaded regions display the range of correlations in $R_{\phi,T}(\rho)$ and $R_{\gamma,T}(\rho)$ from smallest to largest, whereas the darker

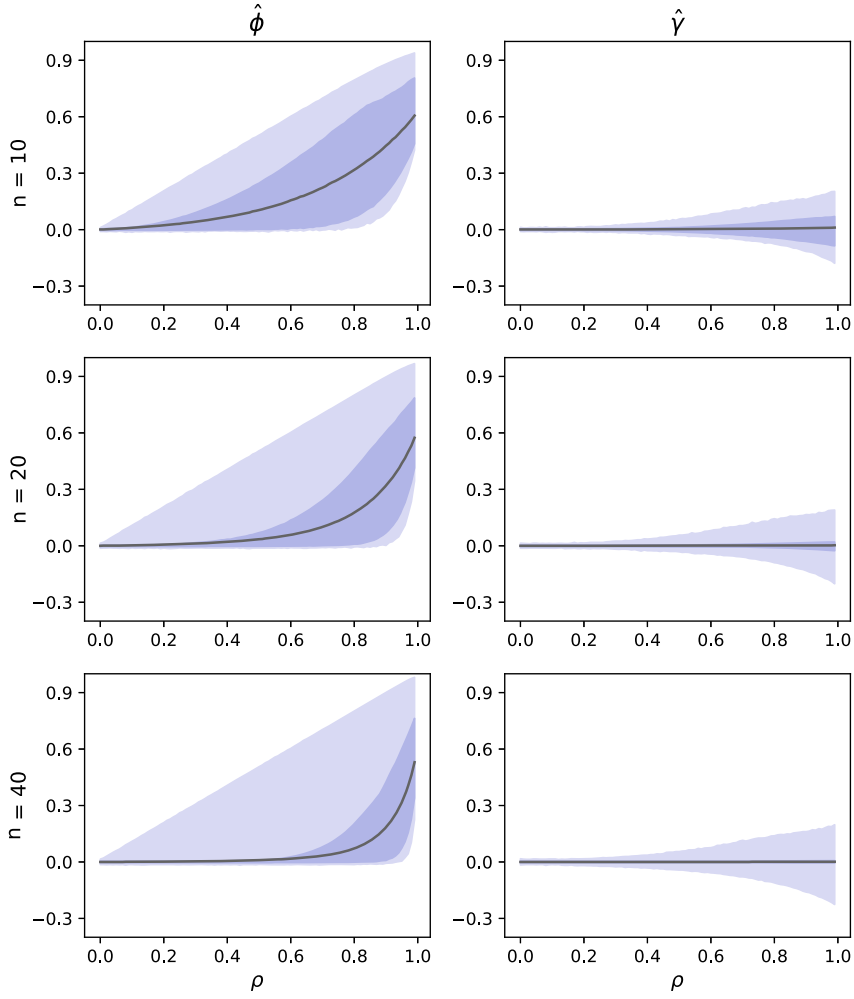

FIGURE S.4.—The solid line is the eigenvalue-based correlation-measures in $R_{\phi,T}(\rho)$ (left panels) and in $R_{\gamma,T}(\rho)$ (right panels), as a function of ρ. The upper, middle, and lower panels are for the case where $\hat{C}$ is an 10×10, 20×20, and 40×40, respectively. The lightly shaded regions display the full range of correlations, whereas the darker shaded regions are defined by the 10%-quantile and 90%-quantile of the off-diagonal elements in $R_{\phi,T}(\rho)$ and $R_{\gamma,T}(\rho)$. Evidently, the elements of $\hat{\gamma}$ are far less correlated than are the elementwise Fisher correlations, $\hat{\phi}$.

shaded regions are defined by the 10%-quantile and 90%-quantile of all the off-diagonal elements in $R_{\phi,T}(\rho)$ and $R_{\gamma,T}(\rho)$.

Figure S.4 also shows that there is far less correlation between the elements of $\hat{\gamma}$ than is the case for the elementwise Fisher transformed variables, $\hat{\phi}$, for all values of ρ. While the correlations between elements of $\hat{\phi}$ are substantially different from zero when ρ approaches one, the correlations between elements of $\hat{\gamma}$ are small and centered about zero. The darker shaded regions include 80% of the correlations, and Figure S.4 shows that the large majority of correlations for $\hat{\gamma}$ are very close to zero, even as ρ approaches 1, whereas the dispersion of the correlations related to $\hat{\phi}$ is much larger. Interestingly, for this design, we see that the correlations between elements of $\hat{\gamma}$ are increasingly concentrated

near zero, as the dimension of C increases. The darker shaded region is barely visible for $\hat{\gamma}$ when $n = 40$. For both $\hat{\phi}$ and $\hat{\gamma}$, we observe that the extreme correlations, (the smallest and largest), are similar for $n = 10$, $n = 20$, and $n = 40$.

APPENDIX S.2: FINITE-SAMPLE PROPERTIES OF $\hat{\gamma}$ WHEN C HAS ARBITRARY (RANDOM) STRUCTURE

The Toeplitz structure used in the previous section is obviously a very particular structure. So it is possible that some of the simulation results are specific to this structure. For this reason, we also consider a design where C has an arbitrary structure. We generate correlation matrices with a random structure by drawing a random vector, $\gamma \in \mathbb{R}^{n(n-1)/2}$, where each element of γ is drawn independently from the uniform distribution on $[-b, b]$ and compute C from γ. The constant b will be chosen to generate C matrices with a desired range of characteristics, specified below.

First, we generate 1000 random 25×25 correlation matrices with $b = 2$. So each element of $\gamma \in \mathbb{R}^{300}$ is drawn independently from the uniform distribution on $[-2, 2]$. For reference, the preimage of $[-2, 2]$ is approximately $[-0.964, 0.964]$ for the Fisher transformation. For each of these 1000 matrices, we compute the asymptotic covariance matrix, $\text{avar}(\hat{\gamma}) = \Omega_\gamma \in \mathbb{R}^{300\times300}$, under the assumption that $\hat{C}$ is computed from i.i.d. vectors with correlation matrix C and finite fourth moments. Under these assumptions, the expression for $\Omega = \text{avar}(\hat{C})$ is given in Neudecker and Wesselman (1990, Theorem 2). In addition, we denote the asymptotic correlation matrix, $\text{acorr}(\hat{\gamma}) = \widetilde{\Omega}_\gamma$, which can be directly obtained from Ω_γ.

We compare the asymptotic expression for Ω_γ with the finite-sample variance matrix of $\hat{\gamma}$, when $\hat{C}$ is computed from Gaussian distributed random vectors, $X_t \sim \text{i.i.d.} N_{25}(0, C)$, $t = 1, \ldots, T$. The finite-sample variance matrix, $\hat{\Omega}_{\gamma,T}$, is computed using 5000 simulations, that is, 5000 realizations of $\hat{C}$, where each $\hat{C}$ is based on either $T = 100$ or $T = 500$ observations of X_t.

We focus on the diagonal elements of Ω_γ and the off-diagonal elements of $\widetilde{\Omega}_\gamma$, separately. The former indicate the extent to which the transformation $\gamma(C)$ is variance-stabilizing, element-by-element, and the off-diagonal elements of $\widetilde{\Omega}_\gamma$ concern the dependence between the elements of $\hat{\gamma}$. In the previous section, the structure of C was given by a single parameter, ρ. The situation is obviously more complex when C has an arbitrary structure. Fortunately, we find that the key properties of Ω_γ are closely tied to the smallest eigenvalue of C, denoted by $\lambda_{\min}$. We therefore present our results stratified by $\lambda_{\min}$. For reference, in case of an equicorrelation matrix, where all correlations have the same value $\rho \geq 0$, the smallest eigenvalue of C is $(1 - \rho)$, regardless of the dimension, $n \geq 2$.

The left panels of Figure S.5 show the range (smallest and largest values) for $\text{avar}(\hat{\gamma}_i)$, $i = 1, \ldots, 300$ as well as the corresponding finite-sample ranges, based on $T = 100$ in the upper panels and $T = 500$ in the lower panels. The right panels in Figure S.5 present the corresponding results for asymptotic correlations between the elements of $\hat{\gamma}$, $\text{acorr}(\hat{\gamma}_i, \hat{\gamma}_j)$, $i, j = 1, \ldots, 300$, $i \neq j$, as well as for the finite-sample correlations. Since $\gamma \in \mathbb{R}^{300}$, the asymptotic covariance matrix, Ω_γ, has 300 diagonal elements and 44,850 distinct off-diagonal elements. When the smallest eigenvalue is not too small the diagonal elements of Ω_γ are all fairly close to one and the off-diagonal are fairly close to zero. The range of variances becomes more disburse as C approaches singularity (as $\lambda_{\min}$ gets smaller). The finite-sample variances have a tendency to be slightly larger than the asymptotic variances when $T = 100$, whereas there is no obvious bias for $T = 500$.

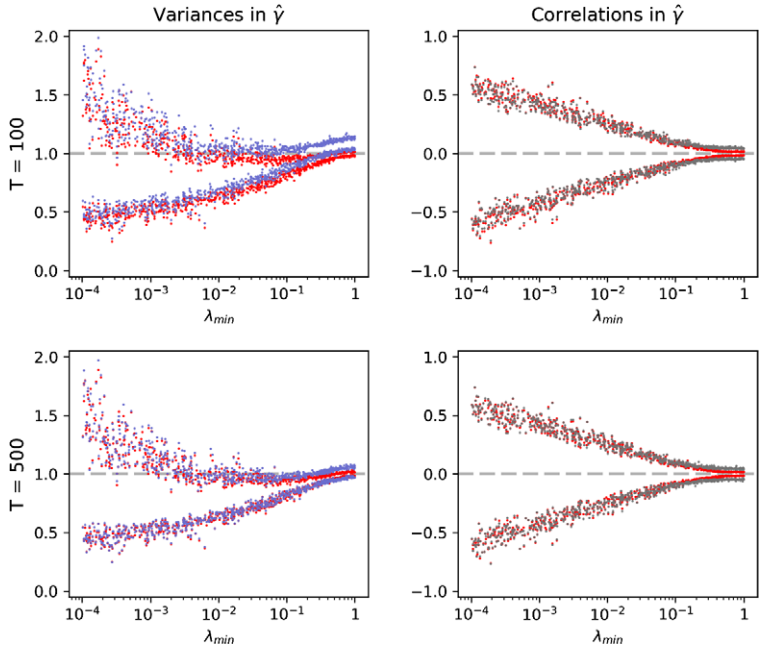

FIGURE S.5.—For each correlation matrix $C \in \mathbb{R}^{25\times 25}$, we compute the corresponding $\Omega_\gamma = \text{avar}(\hat{\gamma})$ and $\widetilde{\Omega}_\gamma = \text{acorr}(\hat{\gamma})$. The left panels present results related to $\text{avar}(\hat{\gamma}_i)$ (diagonal elements of Ω_γ) and the right panels present results related to $\text{acorr}(\hat{\gamma}_i, \hat{\gamma}_j)$ (off-diagonal elements of $\widetilde{\Omega}_\gamma$). The asymptotic range (defined by the smallest and largest elements) is shown with red dots. The corresponding ranges, based on the finite-sample covariance matrix for $\hat{\gamma}$, are presented with blue or gray dots.

APPENDIX S.3: RELATIONSHIP BETWEEN γ AND ϱ

While γ depends nonlinearly on all the elements of C, and vice versa, we have observed that variation in a particular element in $\log C$ primarily influences the corresponding element in C. This suggests that the leading terms in Jacobian $\partial \text{vecl}(C)/\partial \text{vecl}(\log C)$ are the diagonal elements. Indeed, we find this to be the case for these two correlation matrices, and a very similar structure is observed with other correlation matrices (not reported in this paper).

Figure S.6 presents the $\partial\varrho/\partial\gamma$ for the case where C is a 10×10 correlation matrix with the Toeplitz structure and $\rho = 0.9$. The values of each element in $\partial\varrho/\partial\gamma$ are represented by coloring that ranges from -1 (dark blue) to $+1$ (dark red). We also compute $\partial\varrho/\partial\gamma$ for an empirical correlation matrix that is based on 2 years (2018–2019) of daily returns for ten industry portfolios. The industry portfolio returns were downloaded from Kenneth R. French data library. The Jacobian, $\partial\varrho/\partial\gamma$, that corresponds to this 10×10 correlation matrix, is presented in Figure S.7, and the structure of the Jacobian turns to be similar to that based on the Toeplitz structure in Figure S.6.

APPENDIX S.4: SOFTWARE IMPLEMENTATION OF THE ALGORITHM FOR RECONSTRUCTING C FROM γ

Here, we provide software implementation of the algorithm for the inverse transformation, which maps from the real vector space to the space of correlation matrices. The inverse mapping translates any real vector γ of a proper dimensionality to its correspond-

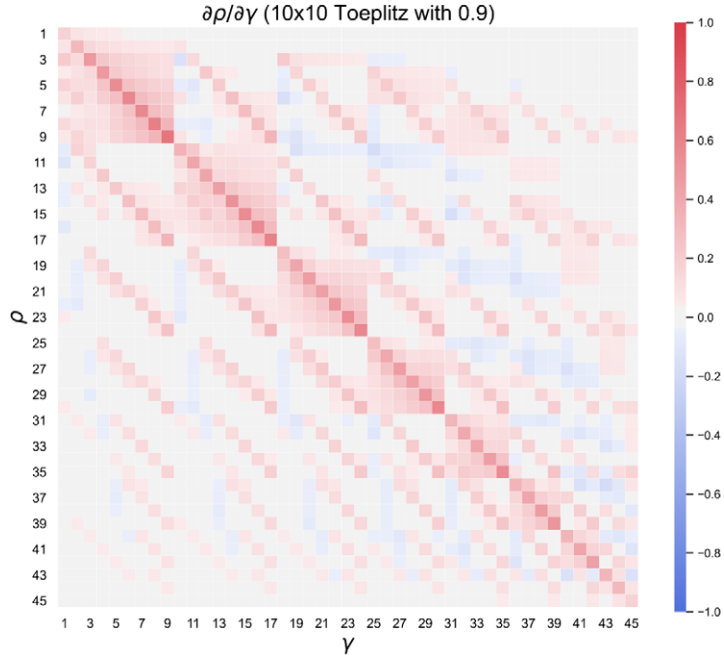

FIGURE S.6.—The Jacobian matrix, $\partial\varrho/\partial\gamma$, for the 10×10 correlation matrix C, when C has a Toeplitz structure $\rho = 0.9$. The value of each element of $\partial\varrho/\partial\gamma$, indicated with a color code, is ranging from -1 (dark blue) to $+1$ (dark red).

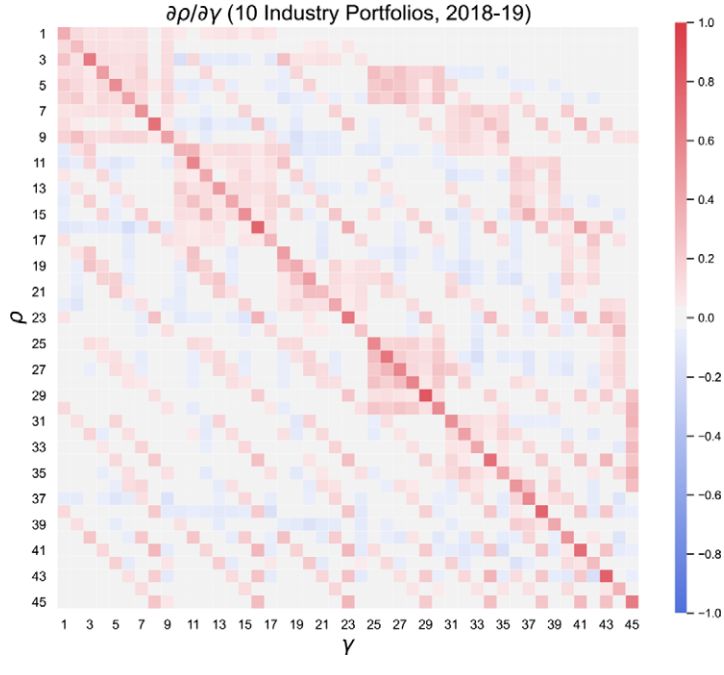

FIGURE S.7.—The Jacobian matrix, $\partial\varrho/\partial\gamma$, evaluated for an empirical correlation matrix C, computed for two years (2018–2019) of daily returns on 10 industry portfolios (available on the Kenneth R. French data library). The value of each element of $\partial\varrho/\partial\gamma$, indicated with a color code, is ranging from -1 (dark blue) to $+1$ (dark red).

ing correlation matrix, $C(\gamma)$, which is unique for any given vector. We provide solutions for the following programming languages: Julia, MATLAB, Ox, Python, and R.

The implementations take the vector γ and a tolerance value, δ, as inputs. First, the dimension of the vector γ is verified as proper (equal to $n(n-1)/2$ for some $n \geq 2$). Then a symmetric matrix $A[x]$ is constructed, where lower and upper off-diagonal parts are filled by the elements of γ, and $x_0 = \text{diag}(A) = 0$ is a vector of starting values for the algorithm. The algorithm iterates over the diagonal vector until the diagonal elements of $e^{A[x^*]}$ are sufficiently close to one, as defined by the tolerance level, which implies that $e^{A[x^*]}$ is close to being a correlation matrix. The algorithm terminates once the vector norm $\|x_{(k)} - x_{(k-1)}\| < \sqrt{n}\delta$, where $x_{(k)}$ is a diagonal vector of the matrix A after kth iteration.

The implementations return the unique correlation matrix, $C = e^{A[x^*]}$, along with the number of iterations that were needed for convergence.

S.4.1. *Julia (Version 1.4)*

```
using Base, LinearAlgebra
function GFT(gam::AbstractArray)
    tol_value=1e-8
    n = 0.5*(1+ sqrt(1+8*length(gam)))
    if (n != floor(n))
        println("Error: Dimension of gamma should be n(n-1)/2x1")
    end
    n = Int(n)
    diag_ind = Matrix{Bool}(I,n,n)
    A = zeros(n,n) # fill matrix A with elements from vector gam
    l = 1
    for j = 1:n-1
        for i = j+1:n
            A[i,j] = A[j,i] = gam[l]
            l += 1
        end
    end
    x = zeros(n) #initial value for diagonal
    dist = n
    iter_number = -1
    while dist > sqrt(n)*tol_value
        Delta = log.(diag(exp(A)))
        x = x - Delta
        A[diag_ind] = x
        dist = norm(Delta)
        iter_number = iter_number + 1
    end
    C = exp(A)
    C[diag_ind] = ones(n) # make diagonal exactly equal to one
    return (C=C, iter_number=iter_number)
end
```

S.4.2. *MATLAB (R2009a Version and Later)*

```
function [C,iter_number] = GFT_inverse_mapping(gamma_in,tol_value)
    C = [];
    iter_number = -1;

    % Check if input is of proper format: gamma is of suitable length
    % and tolerance value belongs to a proper interval
    n = 0.5*(1+sqrt(1+8*length(gamma_in)));
    if isvector(gamma_in) && (n == floor(n))...
        && (tol_value >= 1e-14 && tol_value <= 1e-4)

        % Place elements from gamma into off-diagonal parts
        % and put zeros on the main diagonal of nxn symmetric matrix A
        A = zeros(n);
        A(logical(tril(ones(n),-1))) = gamma_in;
        A = A + A';

        % Read some properties of matrix A
        diag_vec = diag(A);
        diag_ind = logical(eye(n));

        % Iterative algorithm to get the proper diagonal vector
        dist = sqrt(n);
        while dist > sqrt(n)*tol_value
            diag_delta = log(diag(expm(A)));
            diag_vec = diag_vec - diag_delta;
            A(diag_ind) = diag_vec;
            dist = norm(diag_delta);
            iter_number = iter_number + 1;
        end

        % Get a unique reciprocal correlation matrix
        C = expm(A);
        C(diag_ind) = ones(n,1);

    else
        fprintf('Error: input is of wrong format');
    end
```

S.4.3. *OxMetrics*

```
#include <oxstd.h>

GFT_inverse_mapping(const gamma_in, const tol_value){
    decl n, A, diag, dist, diag_delta, iter_number, C;
    iter_number = -1

    // Check if input is of proper format: gamma is of suitable length
    // and tolerance value belongs to a proper interval
    n = 0.5*(1 + sqrt(1+8*rows(gamma_in)));
    if(n != floor(n)){
        print("Dimension of 'gamma' is incorrect"); exit(1);
    }
    if(tol_value < 1e-14 || tol_value > 1e-4){
        print("Incorrect tolerance value"); exit(1);
    }

    // Place elements from gamma into off-diagonal parts
    // and put zeros on the main diagonal of nxn symmetric matrix A
    A = setlower(zeros(n,n),gamma_in);
    A = A + A';

    // Read properties of the input matrix
    diag = diagonal(A)';

    // Iterative algorithm to get the proper diagonal vector
    dist = sqrt(n)
    while(dist > sqrt(n)*tol_value){
        diag_delta = log(diagonal(expm(setdiagonal(A,x))))';
        diag = diag - diag_delta;
        A = setdiagonal(A,diag);
        dist = norm(d,2);
        ++iter_number;
    }

    // Get a unique reciprocal correlation matrix
    C = expm(setdiagonal(A,x))
    C = setdiagonal(C,ones(n,1));

    return {C, iter_number};
}
```

S.4.4. *Python 3 (Using NumPy and SciPy Libraries)*

```python
import numpy as np
from scipy.linalg import expm, norm

def GFT_inverse_mapping(gamma_in,tol_value):
    C = []
    iter_number = -1

    try:
        # Check if input is of proper format: gamma is of suitable length
        # and tolerance value belongs to a proper interval
        n = 0.5*(1+np.sqrt(1+8*len(gamma_in)))
        if not all([gamma_in.ndim == 1, n.is_integer(),
                            1e-14 <= tol_value <= 1e-4]):
            raise ValueError

        # Place elements from gamma into off-diagonal parts
        # and put zeros on the main diagonal of nxn symmetric matrix A
        n = int(n)
        A = np.zeros(shape=(n,n))
        A[np.triu_indices(n,1)] = gamma_in
        A = A + A.T

        # Read properties of the input matrix
        diag_vec = np.diag(A)
        diag_ind = np.diag_indices_from(A)

        # Iterative algorithm to get the proper diagonal vector
        dist = np.sqrt(n)
        while dist > np.sqrt(n)*tol_value:
            diag_delta = np.log(np.diag(expm(A)))
            diag_vec = diag_vec - diag_delta
            A[diag_ind] = diag_vec
            dist = norm(diag_delta)
            iter_number += 1

        # Get a unique reciprocal correlation matrix
        C = expm(A)
        np.fill_diagonal(C, 1)

    except ValueError:
        print("Error: input is of wrong format")

    return C, iter_number
```

S.4.5. *R (Using "Expm" Library)*

```
library(expm)

GFT_inverse_mapping <- function(gamma_in, tol_value){
    C <- matrix(,nrow=0,ncol=0)
    iter_number <- -1

    # Check if input is of proper format : gamma is of suitable length
    # and tolerance value belongs to a proper interval
    n <- 0.5*(1+sqrt(1+8*length(gamma_in)))
    if (!(is.vector(gamma_in) && n%%1==0)){
        stop("Dimension of 'gamma' is incorrect")
    } else if (!(tol_value>=1e-14 && tol_value<=1e-4)){
        stop("Incorrect tolerance value")
    } else {

        # Place elements from gamma into off-diagonal parts
        # and put zeros on the main diagonal of nxn symmetric matrix A
        A <- matrix(0,nrow=n,ncol=n)
        A[upper.tri(A, diag=FALSE)] <- gamma_in
        A <- A + t(A)

        # Read properties of the input matrix
        diag_vec <- diag(A)

        # Iterative algorithm to get the proper diagonal vector
        dist <- sqrt(n)
        while (dist > sqrt(n)*tol_value){
            diag_delta <- log(diag(expm(A)))
            diag_vec <- diag_vec - diag_delta
            diag(A) <- diag_vec
            dist <- norm(diag_delta, type="2")
            iter_number <- iter_number + 1
        }

        # Get a unique reciprocal correlation matrix
        C <- expm(A)
        diag(C) <- rep(1,n)
    }

    return(list(C=C, iter_number=iter_number))
}
```

REFERENCES

FRIEDMAN, S., AND H. F. WEISBERG (1981): "Interpreting the First Eigenvalue of a Correlation Matrix," *Educational and Psychological Measurement*, 41, 11–21. [3]

MORRISON, D. F. (1967): *Multivariate Statistical Methods*. New York: McGraw-Hill. [3]

NEUDECKER, H., AND A. WESSELMAN (1990): "The Asymptotic Variance Matrix of the Sample Correlation Matrix," *Linear Algebra and its Applications*, 127, 589–599. [6]

Co-editor Ulrich K. Müller handled this manuscript.

Manuscript received 18 December, 2018; final version accepted 22 September, 2020; available online 3 December, 2020.